Articles

Yeast Mitochondrial Dehydrogenases Are Associated in a Supramolecular Complex†

Xavier Grandier-Vazeille,*,‡ Katell Bathany,§ Stéphane Chaignepain,‡ Nadine Camougrand,‡ Stéphen Manon,‡ and Jean-Marie Schmitter§

UMR5095 C.N.R.S./Université de Bordeaux 2, 1 rue Camille Saint-Saëns, 33077 Bordeaux Cedex, France, and UMR5472 C.N.R.S./Université de Bordeaux 1, Avenue Pey-Berland, 33405 Talence Cedex, France

Received February 8, 2001; Revised Manuscript Received May 29, 2001

ABSTRACT: Separation of yeast mitochondrial complexes by colorless native polyacrylamide gel electrophoresis led to the identification of a supramolecular structure exhibiting NADH−dehydrogenase activity. Components of this complex were identified by N-terminal Edman degradation and matrix-assisted laser desorption ionization mass spectrometry. The complex was found to contain the five known intermembrane space-facing dehydrogenases, namely two external NADH−dehydrogenases Nde1p and Nde2p, glycerol-3-phosphate dehydrogenase Gut2p, D- and L-lactate-dehydrogenases Dld1p and Cyb2p, the matrix-facing NADH−dehydrogenase Ndi1p, two probable flavoproteins YOR356Wp and YPR004Cp, four tricarboxylic acids cycle enzymes (malate dehydrogenase Mdh1p, citrate synthase Cit1p, succinate dehydrogenase Sdh1p, and fumarate hydratase Fum1p), and the acetaldehyde dehydrogenase Ald4p. The association of these proteins is discussed in terms of NADH-channeling.

The budding yeast *Saccharomyces cerevisiae* is a universal model organism for cellular biology studies. This facultative aerobe is a unique tool for bioenergetic studies, since mutants deficient in mitochondrial functions are still able to grow under fermentative conditions, thus allowing the isolation and study of deficient mitochondria. When grown on a nonfermentable carbon source, such as lactate, yeast mitochondria exhibit a general organization and function very similar to mammalian mitochondria. However, their respiratory chain differs on several aspects.

Opposite to bacteria and mitochondria from most eukaryotes, *S. cerevisiae* mitochondria do not have any rotenone-sensitive NADH-ubiquinone oxidoreductase, identified as respiratory complex I. The mammalian complex is a supramolecular structure composed of at least 40 different subunits, which couples electron transfer from matricial NADH to membrane ubiquinone with a proton translocation from the matrix to the mitochondrial intermembrane space (see ref *1* for review). This lack of complex I partly explains the lower phosphorylation efficiency of yeast mitochondria as compared to mammalian mitochondria, since yeast mitochondria only support two sites of coupling, namely complex III (ubiquinol-cytochrome *c* oxidoreductase) and complex IV (cytochrome *c* oxidase).

Instead of a complex I, yeast mitochondria contain a rotenone-insensitive matrix-facing NADH-ubiquinone oxidoreductase. This enzyme has been purified and is constituted of a single 57 kDa-protein, encoded by the gene *NDI1* (*2*, *3*). The inactivation of this gene results in a slightly altered growth phenotype on carbon sources leading to matricial substrates such as pyruvate, which happens for, e.g., low glucose concentrations.

It is well established that yeast mitochondria are able to oxidize cytosolic NADH via an intermembrane space-facing NADH-ubiquinone oxidoreductase. It has been shown that this activity is supported by two distinct enzymes, encoded by the genes *NDE1* and *NDE2*, identified on the basis of their homology with *NDI1* (*4*, *5*). The deletion of one of the two genes does not impair growth, but the deletion of both genes induces a dramatic reduction of growth rate on most carbon sources under aerobic conditions. These enzymes play a key-role in the regulation of oxidative phophorylation since their activities modulate the electron flow through the respiratory chain and consequently modify both the whole mechanistic H^+/e^- stoichiometry of the respiratory chain (*6*−*8*) and the permeability of the inner mitochondrial membrane (*9*).

In addition to cytosolic NADH, yeast mitochondria are able to oxidize directly other cytosolic substrates. Cytosolic glycerol-3-phosphate can be oxidized by an inner membrane-bound glycerol-3-phosphate-ubiquinone oxidoreductase, encoded by the gene *GUT2*, which, in association with cytosolic enzymes, encoded by *GPD1* and *GPD2* genes, creates a glycerol-3-phosphate shuttle involved in redox adjustment (*10*). Lactate is oxidized by a D-lactate-cytochrome *c* oxidoreductase and a L-lactate-cytochrome *c* oxidoreductase

† This work was supported by grants from the Centre National de la Recherche Scientifique, the Université de Bordeaux 2, the Université de Bordeaux 1, the Ecole Polytechnique and the Conseil Régional d'Aquitaine.

* To whom correspondence should be addressed. Phone: 33-556-99-90-50. Fax: 33-556-99-90-51. E-mail: x.grandier-vazeilles@ibgc.u-bordeaux2.fr.

‡ UMR5095 C.N.R.S.

§ UMR5472 C.N.R.S.

10.1021/bi010277r CCC: $20.00
Published on Web 07/25/2001

encoded by the genes *DLD1* and *CYB2*, respectively (*11*, *12*).

In addition to these peculiar dehydrogenases activities, yeast is also able to realize both cytosolic and mitochondrial bypasses for pyruvate oxidation via acetaldehyde dehydrogenases (*13*−*15*). This large number of possible pathways for NADH reoxidation makes yeast able to grow on a large variety of carbon sources and under a wide variety of conditions.

There are compelling in vitro evidences that, in mammalian mitochondria, a channeling process occurs between the different dehydrogenases (*16*−*19*) and between consecutive enzymes of the TCA[1] cycle such as fumarase and malate dehydrogenase (*20*) or malate dehydrogenase and citrate synthase (*21*, *22*). This channeling is related to probable physical contacts between the enzymes (*23*). It has also been shown that citrate synthase behave as an immobilized protein in vivo, suggesting that it is part of a complex (*24*). In vivo demonstrations of channeling between malate dehydrogenase and citrate synthase (*22*) and citrate synthase and aconitase (*25*) were done in yeast by genetic methods.

It is often considered that the high protein concentration of the mitochondrial matrix limits metabolites diffusion and that channeling is therefore required to overcome diffusive barriers. However, it has been shown that matrix-addressed GFP is able to diffuse rapidly, suggesting that other matrix proteins are organized in membrane-bound complexes, which lets a relatively uncrowded aqueous space allowing the rapid diffusion of metabolites (*26*). These indirect evidences suggest that mitochondrial enzymes are somehow organized into supramolecular complexes, even if it is not clear that this organization plays a role in metabolites channeling.

In a previous study, we separated mitochondrial complexes on the basis of nondenaturing electrophoresis methods (*27*). The complexes were identified by their enzymatic activities. NADH−NitroBlue Tetrazolium oxidoreductase activities were observed, the major one corresponding to a large complex, comparable in size with "classical" mitochondrial complexes such as bc1, cytochrome *c* oxidase and FoF1-ATPase. The goal of the present work was to identify the components of this complex. This was achieved by coupling a first-dimension nondenaturing electrophoresis and a second-dimension denaturing electrophoresis followed by endoproteolysis of discrete bands and analysis of polypeptides by MALDI-MS and microsequencing. We conclude that yeast mitochondrial dehydrogenases are associated into a membrane-bound pseudo-complex. The significance of such an organization for the regulation of mitochondrial metabolism is discussed.

EXPERIMENTAL PROCEDURES

Yeast Strains and Media. The *S. cerevisiae* strains used in this study were the parental haploid strain W303-1B (*MATa*, *ade2*, *his3*, *trp1*, *leu2*, *ura3*, *canR*) and derivatives of this strain containing specific gene disruption. These include strains containing disruptions of the *NDI1*, *NDE1*, *NDE2*, and *GUT2* loci, constructed as follows. The *NDI1*, *NDE1*, and *NDE2* genes were amplified by PCR using the following primers: 5′-GTGGGGAGCTATTTCGTTTT-3′ and 5′-TTAAGGAAGTACTCTCCCGA-3′ for *NDI1*, 5′-GTCTTGCCAAGTCTCTTTGA-3′ and 5′-GTGTGACATCGTTGCTGTTT-3′ for *NDE2* and 5′-TTGCATTCACAACCATCACC-3′ and 5′-GCGCTTTCTCTTCGATTCAT-3′ for *NDE1*. PCR fragments were further cloned in the pGEM-Easy vector (Promega). These plasmids were used to construct the Δ*ndi1::TRP1*, Δ*nde1::URA3*, and Δ*nde2::LEU2* strains. For *NDI1*, a 1032 bp HindIII digestion fragment was replaced by the full *TRP1* gene from pFL39 plasmid. For *NDE1*, a 700 bp *Nar*I−*Age*I digestion fragment was replaced by the full *URA3* gene from pFL38 plasmid. For *NDE2*, a 1236 bp *Bgl*II digestion fragment was replaced by the full *LEU2* gene from pFL46L plasmid. An *Eco*R1-digestion fragment from each construction was used to transform the W303-1B strain. All constructions were then confirmed by PCR.

The strain containing the *GUT2* disruption was provided by Professor Lena Gustafsson (University of Göteborg, Sweden) and was constructed as described in (*10*). The double mutant for *NDE1* and *NDE2* was constructed by disrupting *NDE2* in the *NDE1*-less strain.

All cells were grown aerobically on a complete medium (1% Yeast Extract, 0.1% potassium phosphate, 0.12% ammonium sulfate, pH 5.0) supplemented with 2% DL-lactate and harvested in mid-exponential growth phase.

In Situ NADH Dehydrogenase Activity. Cells harvested in mid-exponential growth phase were converted to spheroplasts as described in ref *8*. Permeabilization of the plasma membrane was done by incubating spheroplasts (1 mg/mL) in a 10 mM potassium phosphate buffer (pH 7.2) containing 1 M sorbitol, 10 mM NH_4Cl, 10 mg/mL bovine serum albumin, and 50 μg/mL nystatin (Sigma) in the cell of an oxygraph. After a 10 min permeabilization, NADH production by glycolysis was induced following the addition of 5 mM fructose-1−6-diphosphate, 1 mM ADP, and 8 mM NAD^+. NADH-linked oxygen-consumption rate was measured at steady state.

Cytochrome Content. Cells were grown aerobically until mid-exponential growth phase and 100 mL of cultures were harvested and washed twice with distilled water. Cells suspensions were adjusted at 70 OD_{550nm} units and were dispatched in the cuvettes of a double-beam spectrophotometer (Aminco DW2000). The reference cuvette content was oxidized by adding 1 μL of hydrogen peroxide, and the sample cuvette content was reduced by adding several crystals of sodium dithionite. Difference spectra were acquired between 500 and 650 nm. Cytochromes $a + a_3$, *b*, and *c* were measured from the absorbance differences at 603 minus 630 nm ($\epsilon = 12\,000\ M^{-1}\ cm^{-1}$), 561 minus 575 nm ($\epsilon = 18\,000\ M^{-1}\ cm^{-1}$) and 550 minus 540 nm ($\epsilon = 18\,000\ M^{-1}\ cm^{-1}$), respectively. Dry weights were measured after drying 1 mL of the same suspension at 180 °C for 3 days in a Pasteur Owen, and weighting the dry residue.

Samples Preparation and Native Electrophoresis. Mitochondria isolated from spheroplasts according to ref *28* were sedimented by centrifugation (12500*g*, 10 min). Mitochondria were further washed twice with 0.75 M ϵ-aminocaproic acid,

[1] Abbreviations: BN-PAGE, blue native polyacrylamide gel electrophoresis; BSA, bovine serum albumin; CN-PAGE, colorless native polyacrylamide gel electrophoresis; GFP, green fluorescent protein; MALDI-MS, matrix-assisted laser desorption ionization mass spectrometry; PCR, polymerase chain reaction; PSD, postsource decay; SDS−PAGE, sodium dodecyl sulfate polyacrylamide gel electrophoresis; TCA cycle, tricarboxylic acids cycle; TFA, trifluoroacetic acid.

50 mM bis-Tris (pH 7.0). They were suspended at 10 mg/mL in the same buffer, solubilized with Triton X-100 as indicated in the text, centrifuged for 20 min at 105.000*g* to remove unsolubilized material, and submitted to first-dimension CN−PAGE as described previously (*27*), except that the detergent/protein ratio was 0.7 or 2.5, as indicated in the legends to figures. Specific staining for NADH dehydrogenase activities was done in a 100 mM Tris/glycine buffer at pH 7.4 containing 0.1 mg/mL nitroblue-tetrazolium (Sigma) and 100 μM β-NADH.

Two-Dimensional SDS−PAGE and Protein Detection. Analysis of the composition of native protein complexes was done by slicing the stained lane of interest (~3 × 165 mm) from the CN−PAGE, which was further treated and subjected to 12.5% tricine-SDS−PAGE as described previously (*27*). Fixation and staining of proteins in 2D-SDS gels were done overnight with 0.03% Amido Black in 45% (v/v) methanol, 10% (v/v) acetic acid. Stained protein bands were cut out and washed in a large volume of water to remove acetic acid and methanol.

In-Gel Protein Digestion. Stained bands of interest were put into 1.5 mL Eppendorf tubes and washed twice with 50% acetonitrile in 25 mM Tris-HCl (pH 8.6) for 30 min at 29 °C. The gel was sliced into small cubes (~1 × 1 × 0.75 mm) and partially dried under vacuum in a SpeedVac concentrator. The gel was rehydrated in digestion buffer (0.1 M Tris-HCl, pH 8.6; 10% acetonitrile) containing 5 μg/mL of endoproteinase Lys-C (Boehringer) in the presence or the absence of 0.03% SDS. After absorption of the protease-containing solution, a minimum volume of digestion buffer was added to totally immerse gel pieces. The digestion was carried out for 18 h at 35 °C and stopped by adding 1/10 vol of 10% TFA in water and mixing. The digestion solution was saved and resulting peptides were recovered by two cycles of washing with 0.1% TFA and extraction by 60% acetonitrile, 0.1% TFA in water (*29*). The digestion solution and supernatants were pooled and concentrated in a SpeedVac.

Reversed-Phase HPLC Peptide Purification. The peptide mixture was fractionnated using an Applied Biosystems 130A HPLC equipped with an Aquapore DEAE ion exchange precolumn (2.1 × 30 mm) and a reverse-phase narrow-bore column Vydac C18 (2.1 × 250 mm) connected in series. Solvent A was 0.1% TFA in water and solvent B was 0.09% TFA in 80/20 acetonitrile/water (v/v). A linear gradient (3% B to 60% B over 57 min) was developped at 0.1 mL/min for peptides elution. The absorbance of the eluate was monitored at 214 nm and peaks were collected manually in 1.5 mL Eppendorf tubes and concentrated to 50 μL in a SpeedVac.

Structural Characterization. N-terminal sequence analyses were done on a gas-phase automatic sequencer (Applied Biosystems 470A) and phenylthiohydantoin-amino acids were identified with an on-line HPLC system. Sequence cycles were run according to the standard protocol provided by the manufacturer. The resulting sequences were identified by searching in the Yeast Proteome Database (http://www.proteome.com/databases/YPD/YPDsearch-seq.html). All sequences considered gave a unique unmismatched answer.

Mass Spectrometry. Prior to mass spectrometry analysis, a micro-chromatographic separation step of proteolytic digests was performed by means of C18 ZipTips (Millipore), using a 10 μL sample load. Two fractions were eluted with 3 μL of solvent (30 and 70% acetonitrile in 0.1% TFA, respectively).

α-Cyano-4-hydroxy-cinnamic acid was used as a matrix, prepared as a saturated solution in 50% acetonitrile/0.1% TFA. Samples were prepared with the dried droplet method on a stainless steel target for 26 samples. External calibration was achieved with a mixture of eight peptides having masses ranging from 1060 (bradykinin) to 3495 Da (β-chain of oxidized bovine insulin). Spectra were acquired with a Bruker Reflex III instrument at 20 kV acceleration voltage and at 24 kV reflector voltage. For PSD experiments, the reflector voltage was stepped down in 10 to 12 steps, starting from 30 kV, to collect fragment ions from precursor to immonium ions.

Database Searching. Measured monoisotopic mass values were used with a 0.15 Da tolerance to search the NCBI database with the Protein Prospector MSFit search engine (http://falcon.ludwig.ucl.ac.uk), by restricting the species to *S. cerevisiae*. The maximum number of allowed missed cleavages was set to 1. Confirmation of protein identifications was obtained by means of the Protein Prospector MSTag search engine, using mass values of fragment ions obtained from PSD spectra. Input mass values were monoisotopic for the precursor ions and average for fragment ions.

Table 1: NADH-Linked Respiration in Permeabilized Spheroplasts[a]

strains	nmol of O_2 min^{-1} (mg of proteins)$^{-1}$
wild-type	25.8 ± 2
ΔNDE1	24.5 ± 2
ΔNDE2	27.0 ± 1.5
ΔNDE1/ΔNDE2	10.8 ± 4

[a] Cells were grown until mid-exponential growth phase and spheroplasts were prepared according to ref *8*. Cells were suspended at 1 mg/mL in a 10 mM phosphate buffer (pH 7.2) containing 1 M sorbitol, 10 mM NH_4Cl, 10 mg/mL BSA, and 50 μg/mL nystatin. after an 8-min permeabilization, 8 mM NAD^+, 1 mM ADP, and 5 mM fructose-1−6-diphosphate were sequentially added and oxygen consumption was measured with a clark electrode. Data are means of four independent experiments ± sd.

RESULTS

Identification of NADH-Dehydrogenase by CN−PAGE. NADH−dehydrogenase activities were measured in situ, in parental, Δ*nde1*, Δ*nde2*, and Δ*nde1*/Δ*nde2* strains. As reported in Table 1, individual mutants did not exhibit any decrease of NADH−dehydrogenase activities following addition of the NADH-generating system. Only the double mutant exhibited a 50−60% decrease of respiration rate. The remaining activity may correspond to the activity of the matrix-facing dehydrogenase.

Cytochrome spectra showed that the absence of external dehydrogenases induced only a slight decrease of the amount of complex IV (by 10%), measured as the amount of cytochromes $a + a_3$ and a larger decrease of the amounts of cytochrome *c* (by 30%) and of complex III (by 35%), measured as the amount of cytochrome *b* (Table 2). This behavior has often been reported for different mutants of the respiratory chain (*30*), and might be an indication of a co-regulation of functionnally related enzymes, such as NADH−dehydrogenases, which reduced ubiquinone, and complex III, which oxidizes ubiquinol.

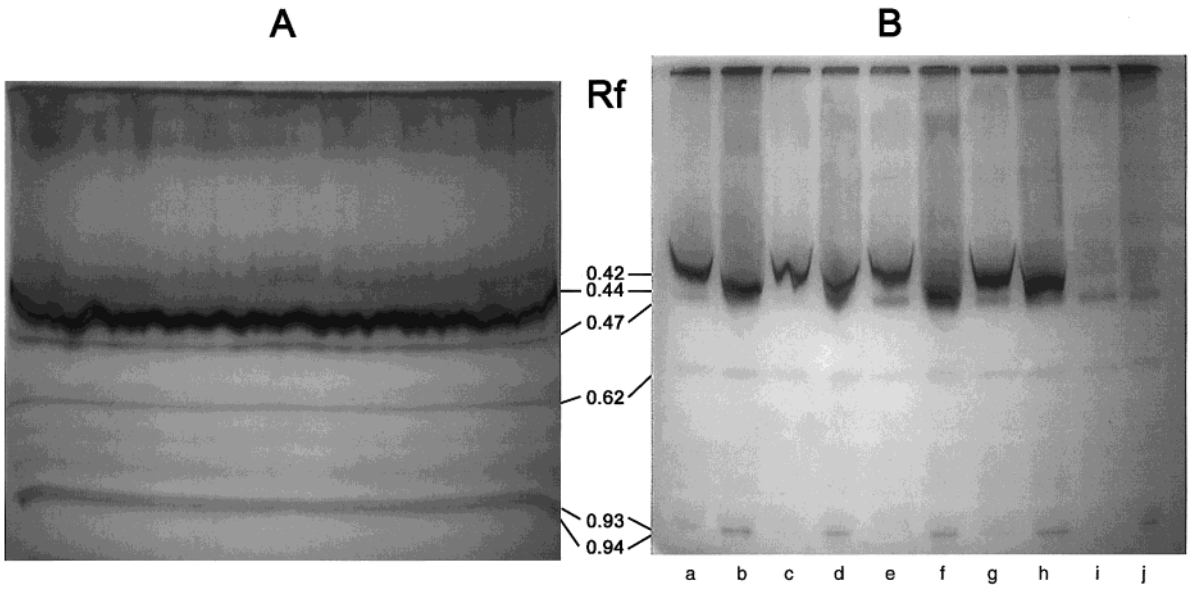

FIGURE 1: Resolution of Oxidative Phosphorylation complexes by one-dimensional CN−PAGE. Supernatants of yeast mitochondria solubilized by Triton X-100 (detergent/protein = 2.5 w/w) were separated on a gradient slab gel (5−14% acrylamide). NADH−dehydrogenase activity was detected as a blue-colored spot on the gel after incubation in a 100 mM Tris/glycine buffer (pH 7.4) containing 0.1 mg/mL Nitro-Blue tetrazolium and 0.1 mM NADH, as described in ref *27*. (A) Supernatants after solubilization of 5 mg of mitochondrial proteins from wild-type strain W303-1B, showing the different stained bands. (B) Comparison between wild-type strains W303-1B (a−d), Δ*nde1* (e−f), Δ*nde2* (g−h), and Δ*nde1*/Δ*nde2* (i−j). Proteins of 0.32 mg (a, c, e, g, i) or 0.56 mg (b, d, f, h, j) were solubilized and submitted to electrophoresis.

Table 2: Cytochrome Content[a]

strains	pmol (mg of dry weight)$^{-1}$		
	cytochrome $a + a_3$	cytochrome b	cytochrome c
wild-type	4.2 ± 0.6	18.9 ± 0.8	36.8 ± 7.7
ΔNDE1	3.5 ± 0.2	12.4 ± 1.1	27.0 ± 3.7
ΔNDE2	3.7 ± 0.6	12.8 ± 1.4	26.3 ± 3.1
ΔNDE1 ΔNDE2	3.8 ± 0.5	11.0 ± 2.0	26.5 ± 5.3

[a] Cells were grown until mid-exponential growth phase, and 100 mL of cultures were harvested and washed twice with distilled water. Cytochrome content was measured as indicated in the Experimental Procedures. Data are means of three independent experiments ± sd.

Preliminary data on the solubilization of a NADH−dehydrogenase complex had been obtained on mitochondrial membranes isolated from a wild-type strain (*27*). Mitochondrial membrane proteins had been suspended at 10 mg/mL and solubilized with Triton X-100 at a detergent/protein ratio of 0.7. These conditions had already been used to vizualize the dimeric form of FoF1-ATP synthase (*27*). After separation on CN−PAGE and staining for NADH dehydrogenase activity, a large band with an R_f of 0.5 was depicted (*27*). Other detergents were assayed, namely lauryl-maltoside, which led to higher R_f bands with weak NADH−dehydrogenase activity (*27*), suggesting that, opposite to Triton X-100, these detergents did not preserve the arrangement of the NADH−dehydrogenase complex.

To achieve a better resolution of this band, the Triton X-100/protein ratio was increased up to 2.5. Mitochondrial membrane proteins from the parental strain were solubilized, separated on CN−PAGE and stained under these conditions. The gel shown in Figure 1 revealed four faint NADH-specific oxidizing activities bands having R_f of 0.47, 0.62, 0.93, and 0.94, respectively, and one high-activity band at $R_f = 0.44$. The mobility of this band was slightly decreased ($R_f = 0.42$) when half reduced the protein load. This high-activity band was present in individual Δ*nde* mutants but was absent in the Δ*nde1*/Δ*nde2* double mutant, showing that it actually contains both external NADH−dehydrogenases.

Identification, by Edman degradation, of the components of the high NADH−dehydrogenase activity proteic band in Δgut2 strain.

Preliminary studies with parental strain and Δ*gut2* mutant solubilized with Triton X-100, at a detergent/protein ratio of 0.7, had shown that the major band exhibiting Glycerol-3-phosphate dehydrogenase activity had the same R_f as the major band exhibiting NADH dehydrogenase activity (data not shown). Initial studies were then performed with Δ*gut2* mutant since our aim was to identify NADH−dehydrogenases. The major band ($R_f = 0.44$) was resolved by Tricine-SDS−PAGE in the second dimension and stained by amido-black, to reveal the subunit composition of the native protein complex (Figure 2A). Twelve bands were detected and analyzed, five with apparent molecular masses ranging between 52 and 64 kDa, three between 39 and 52 kDa, and four between 26 and 39 kDa. Bands were excised and digestion carried out in the gel with endoproteinase Lys-C. The resulting peptide mixtures, dissolved in a total volume of 40 μL, were separated by reversed-phase HPLC (Figure 3) on a narrow-bore C18-column with an anion exchange precolumn in series, to trap SDS and amido-black stain (*31*).

Several major and minor fractions taken from symmetrical peaks from separated digests were submitted to automatic Edman degradation and the corresponding peptide sequences were determined. These sequences were searched in the Yeast Proteome Database and were found to correspond to 10 different proteins (Table 3). Eight are mitochondrial proteins (Sdh1p, Nde1p, Hsp60p, Cyb2p, Dld1p, Fum1p, Om45p, Mdh1p). One is a major cytosolic enzyme (Ach1p) known to contaminate most cellular fractions and one is the product of an unidentified ORF (*YML128C*). No products were found corresponding to *NDI1* or *NDE2* gene.

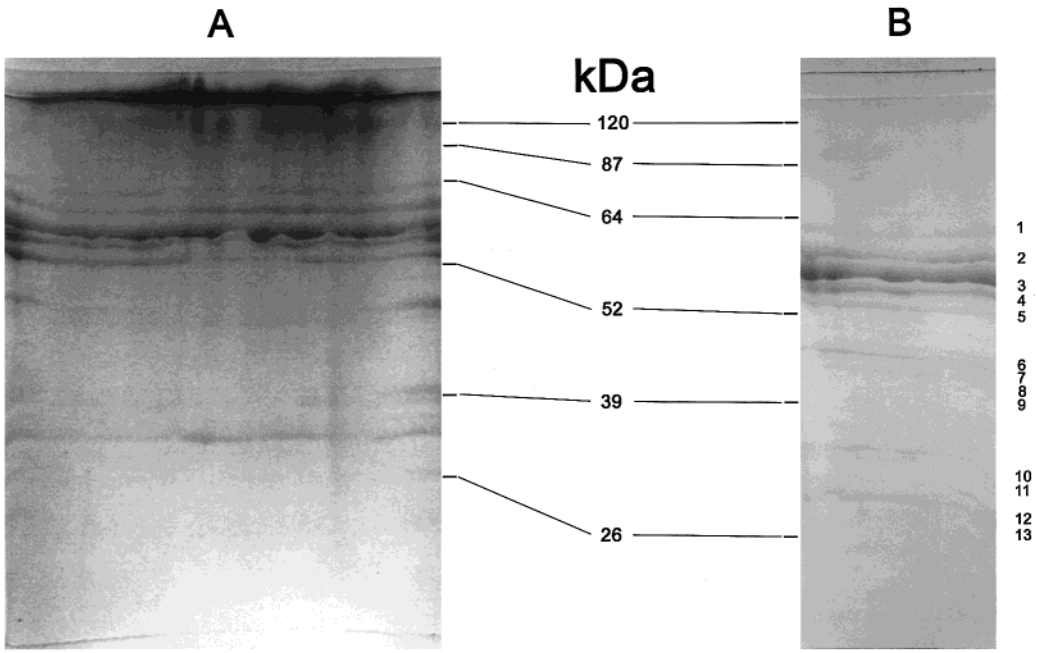

FIGURE 2: Second-dimension analysis of the $R_f = 0.44$ band. The major band having NADH−dehydrogenase activity was submitted to denaturating electrophoresis on tricine-SDS−PAGE (14% T, 3% C), as described in ref *27*. Protein separation was followed using prestained molecular weight markers (SDS-7B, Sigma). The gel was fixed and stained with 0.03% amido black in 45% methanol, 10% acetic acid (v/v). Stained bands (numbered on the right) were cut out and soaked in a large volume of water to remove acetic acid and methanol before further in-gel protein digestion by endoproteinase Lys-C. (A) Components of the complex from Δ*gut2* mitochondria solubilized at a detergent/protein ratio of 0.7. (B) Components of the complex from wild-type mitochondria solubilized at a detergent/protein ratio of 2.5.

Table 3: Identification of Proteins by Edman Degradation of Endoproteinase Lys-C Digestion of Discrete Bands[a]

gene	protein	localization	sequence	position	band
SDH1	succinate dehydrogenase	mitoch. (Mat)	KDVAAPVTL	607−615	2
NDE1	external NADH dehydrogenase	mitoch. (IM)	KNQIV	476−480	2
HSP60	major mitochondrial chaperone	mitoch. (Mat)	KFGVEGR	28−34	3
			KTNXXAXDXTTSATVL	101−116	
			VIEFLS	147−153	
			KASRVLDE	443−450	
			KSEYTDML	507−514	
CYB2	L-lactate dehydrogenase	mitoch. (IM)	KLDMNK	83−90	4
			KARTVGP	564−571	
DLD1	D-lactate dehydrogenase	mitoch. (IM)	KTDPNE	576−581	4
ACH1	acetyl-coA hydrolase	cytosol	KVIIEVNT	174−181	4
YML128C	unknown	?	KYAID	49−53	5
			KDLQNXLNDN	171−180	
			KWSXDQLTNW	241−250	
FUM1	fumarate hydratase	mitoch. (Mat)	KYWGAQTQR	44−52	6
OM45	major outer membrane protein	mitoch. (OM)	KAIAIGEF	129−136	8
			KRLDELK	251−257	
MDH1	malate dehydrogenase	mitoch. (Mat)	KGVATDLS	55−62	8

[a] The known localization of the proteins is indicated. For mitochondrial proteins, the sub-localization is also indicated (inner membrane, outer membrane, matrix). The "Band" column refers to the position of bands in Figure 2.

Since this method resulted in the identification of a low number of proteins, the next step was to use the parental strain, instead of Δ*gut2* and another identification technique.

Identification, by mass spectrometry, of the components of the high NADH−dehydrogenase activity proteic band in parental strain.

During the course of this work, it has been observed that the absence of the external glycerol-3-phosphate dehydrogenase (encoded by the *GUT2* gene) led to alterations in the activities of external NADH−dehydrogenases.[2] To avoid possible side effects linked to *GUT2*-disruption, the following work was done on the parental strain.

In-gel endoproteinase Lys-C digests of bands, excised from the second dimension SDS−PAGE, were systematically treated on reversed phase chromatographic support, using C18-phase packed in pipet tips (ZipTips, see Experimental Procedures). In addition to a desalting and residual acrylamide removal step, this treatment was used to simplify the digests, by separating the complex mixtures in two fractions according to increasing hydrophobicity. This procedure facilitated the identification of proteins present in the stained bands, which rarely corresponded to a single constituent. Identification of proteins was first attempted by searching the NCBI database by means of peptides masses measured from monoisotopic species. Top ranked candidates were checked individually by a systematic PSD mass analysis from

[2] M. Rigoulet, personnal communication.

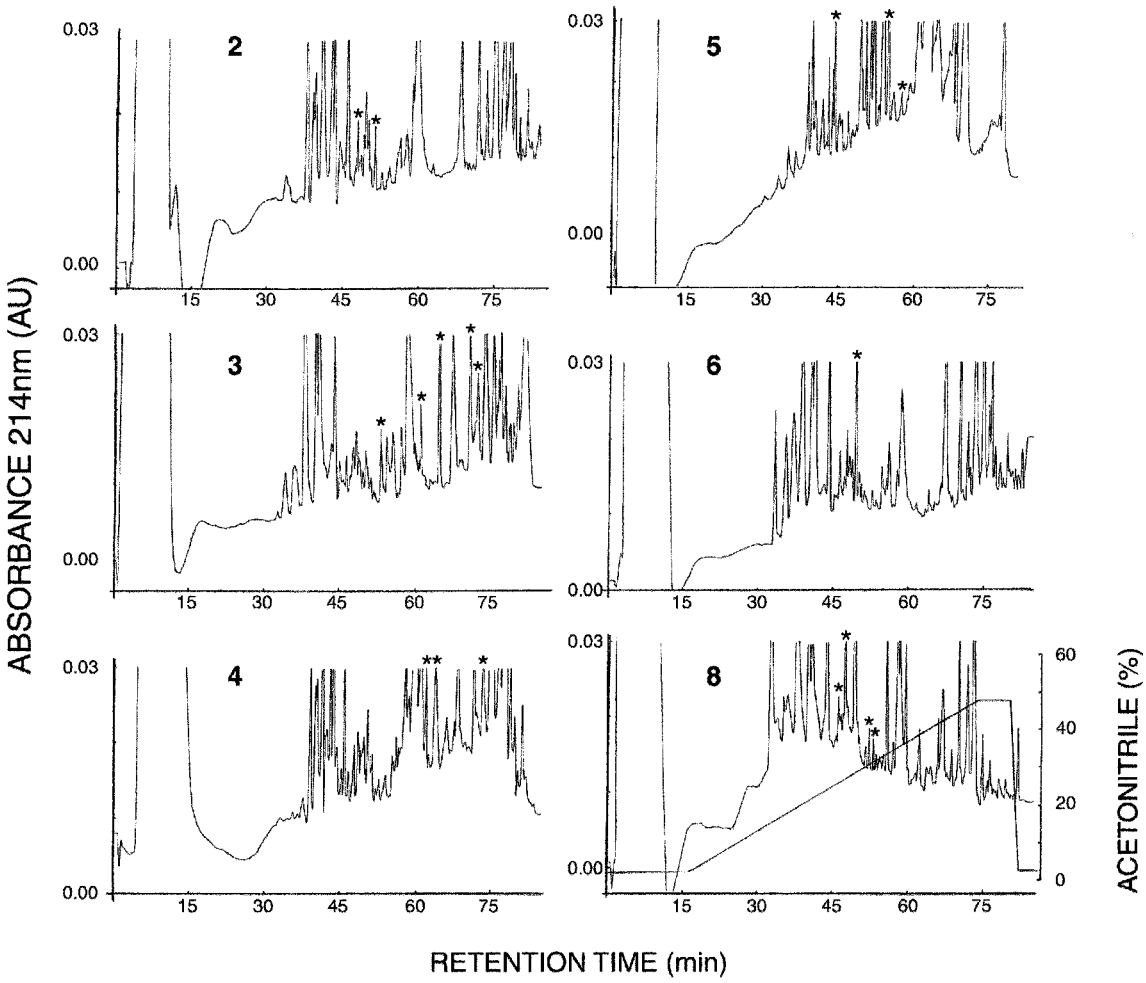

FIGURE 3: Fingerprints of selected bands in Figure 2A. The resulting peptides from endoproteinase Lys-C in-gel digestion of the indicated bands were separated on a reverse-phase narrow bore Vydac C_{18} column (2.1 × 250 mm) connected in series with a DEAE anion exchange precolumn (Aquapore AX300). Elutions were performed at 0.5 mL/min using a 57 min gradient of 3 to 48% acetonitrile in 0.1 to 0.09% TFA. Asterisks indicate peptide peaks for which N-terminal sequence analysis was carried out (see Table 3).

selected signals. Identifications reported below were only considered as definitive when the two separate search procedures (i.e., MSFit and MSTag tools from Protein Prospector) led to a unique answer. A typical mass spectrometry analysis is given in Figure 4, for the product of *NDE2*.

Several components were detected in the digests of each band by mass spectrometry (Table 4). For example, band 3 (see Figure 2B) contained five components, namely glycerol-3-phosphate dehydrogenase Gut2p, mitochondrial chaperone Hsp60p, citrate synthase Cit1p, probable flavoprotein YOR356Wp, and internal NADH dehydrogenase Ndi1p.

A total of 38 proteins were identified (Table 4). Eighteen were found at least five times in three independent experiments. Among them, 14 are known or probable mitochondrial proteins (Hsp60p, Gut2p, Tom70p, Cyb2p, YOR356Wp, Ald4p, Nde2p, OM45p, Ndi1p, Put2p, Cit1p, Mdh1p, Qcr2p, YLR089Cp), one is the product of an unknown ORFs (YML128Cp), two are proteins known as major contaminants of all cellular fractions (Ach1p, Sso1p) and one is a cytoskeleton-associated protein the localization of which is unclear (Bzz1p).

Twenty additional proteins were found less than five times. Seven are known or probable mitochondrial proteins (Qcr1p, Fum1p, Dld1p, Atp1p, YPR004Cp, Idh2p, Mrf1p), seven are major cellular proteins known as contaminants of most cellular fractions (Sso2p, Pgk1p, Sti1p, Eno1p, Tdh3p, Tdh1p, Gpm2p), five are nuclear proteins which are likely to contaminate mitochondria (Mag1p, Nsp1p, Pus1p, Upf3p, Pch2p); one is a cell wall protein and its possible presence in mitochondria will be discussed (Gas1p).

Obviously, the MALDI-MS method led to a much higher number of identifications than the sequencing method but both approaches led to the identification of a common set of proteins: Hsp60p, OM45p, Cyb2p, Dld1p, Mdh1p, Fum1p, YML128Cp, Ach1p. The Edman sequencing method allowed the identification of two proteins (Nde1p, Sdh1p) that were not unambiguously identified by MALDI-MS. Several minor peaks corresponding to peptides derived from these two proteins were observed within some mass spectra but, in these cases, PSD experiments were unsuccessful to confirm their presence because of the limiting resolution of the ion gating system of our mass spectrometer.

DISCUSSION

Inner-Membrane-Bound External Dehydrogenases. This paper gives further evidences for a supramolecular association of mitochondrial dehydrogenases. The enzyme buffering method has provided a large number of evidences for kinetic channeling between mitochondrial enzymes. The kinetic

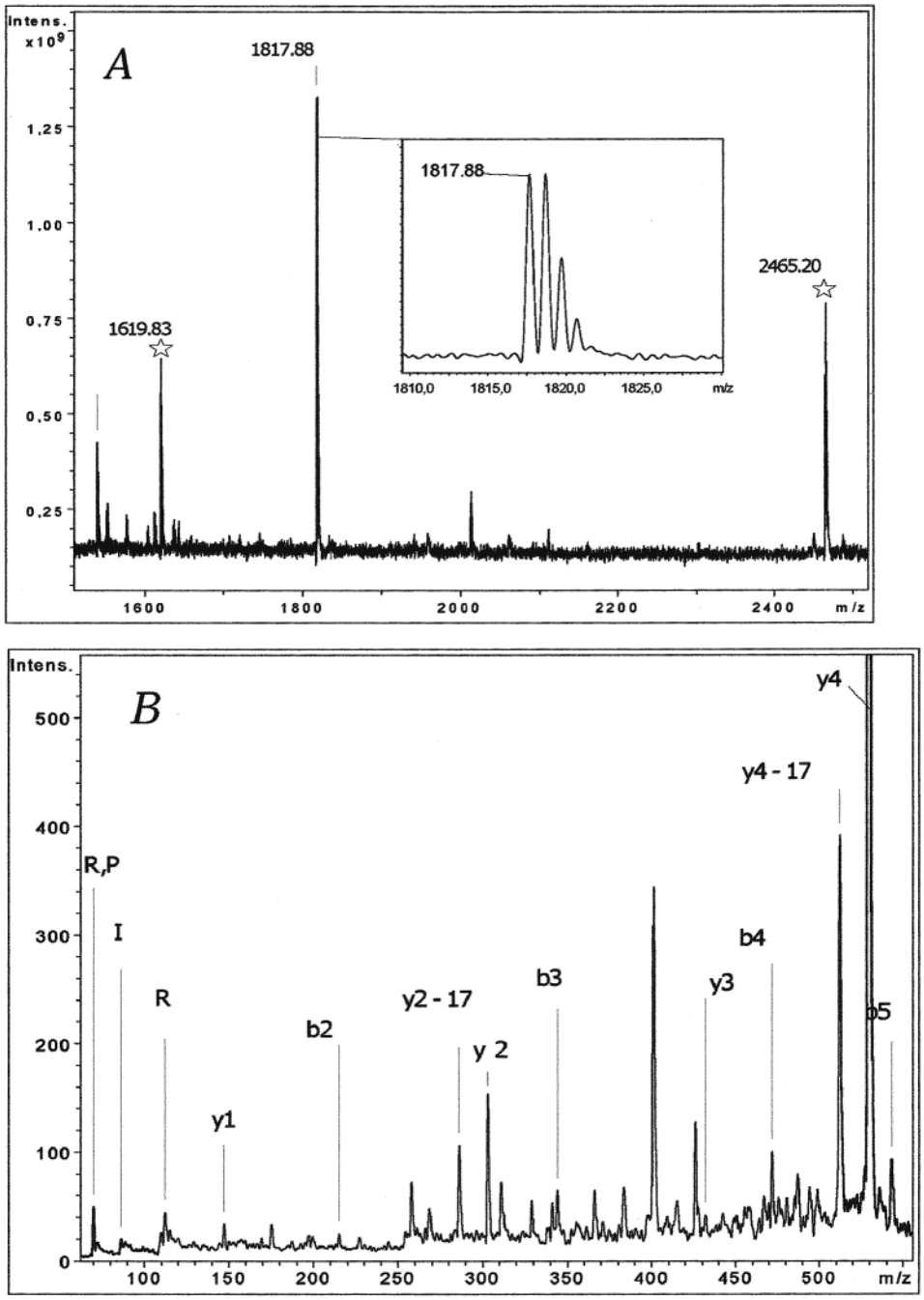

FIGURE 4: Typical example of mass spectrometry identification. (A) MALDI mass spectrum showing a peptide at *m*/*z* 1817.88 belonging to Nde2p bracketed by two internal standards (bombesin at 1619.83 Da and human adrenocorticotropic hormone fragment 18−39 at 2465.20 Da); the monoisotopic peak (inset) matches the theoretical value (1817.90 Da). (B) Partial MALDI PSD spectrum of peptide peak at *m*/*z* 1817.88, with identified N-terminal (b type), C-terminal (y type), and immonium ions confirming the sequence TIEQASSFPVNDPERK of this peptide belonging to Nde2p.

advantage of "organized enzymes" vs "fully soluble" enzymes of the TCA cycle has been clearly demonstrated (*21*). On the other hand, direct evidences for physical contacts between enzymes of the TCA cycle were only obtained for peculiar enzymes: binding of malate dehydrogenase to complex I in beef heart mitochondria (*19*), and channeling of malate dehydrogenase and citrate synthase (*22*) and of citrate synthase and aconitase in yeast mitochondria (*25*). In addition, the observation that citrate synthase behaves as an immobilized enzyme suggests its participation to a supramolecular complex (*24*).

In addition to matricial enzymes, it is well described, for instance, that defects in the yeast FoF1-ATPase complex induce assembly defects of the bc1 and cytochrome *c* oxidase complexes (*30*). A supramolecular organization of the complexes involved in oxidative phosphorylation has been shown by nondenaturating electrophoresis methods (*32*). Concerning dehydrogenases, it has been observed that the inactivation of *GUT2* (encoding the mitochondrial glycerol-3-phosphate ubiquinone oxidoreductase) induces a modification of the kinetic parameters of intermembrane space-facing NADH-ubiquinone oxidoreductase.[2]

Table 4: MALDI-MS Identification of the 38 Proteins Found in the Band at $R_f = 0.44$[a]

gene	protein	size	band (Figure 3B)	localization	no. of Identifications
HSP60	major mitochondrial chaperone	58 249	3	mitoch. (Mat)	74
GUT2	glycerol-3-phosphate dehydrogenase	68 435	2	mitoch. (IM)	43
TOM70	mitochondrial proteins receptor	70 109	1	mitoch. (OM)	25
CYB2	L-lactate dehydrogenase	56 584	4	mitoch. (IM)	20
YOR356W	probable flavoprotein	69 504	1	mitoch.?	14
ALD4	acetaldehyde dehydrogenase	53 967	4	mitoch. (Mat)	12
NDE2	external NADH-dehydrogenase	61 662	4	mitoch. (IM)	12
YML128C	unknown	59 587	5	?	11
ACH1	acetyl-coA hydrolase	58 573	4	cytosol	10
OM45	major outer-membrane protein	44 452	13	mitoch. (OM)	9
NDI1	internal NADH-dehydrogenase	54 260	3	mitoch. (IM)	8
PUT2	Δ1-pyrroline 5-carboxylate dehydrogenase	61 157	4	mitoch. (IM)	7
BZZ1	cytoskeleton-associated protein?	71 027	2	?	7
CIT1	citrate synthase	49 038	7	mitoch. (Mat)	6
MDH1	malate dehydrogenase	33 831	13	mitoch. (Mat)	6
QCR2	complex III core protein	38 702	10	mitoch. (IM)	5
SSO1	ER membrane major component	32 962	11	ER	5
YLR089C	probable alanine aminotransferase	66 416	5	mitoch. (Mat)	5
SSO2	ER membrane major component	33 585	11	ER	3
QCR1	complex III core protein	47 402	8	mitoch. (IM)	2
FUM1	fumarate hydratase	50 125	6	mitoch. (Mat)	2
MAG1	DNA-3-methyladenine hydroxylase	34 335	12	nucleus	2
PCH2	probable ATPase	63 315	3	nucleus	2
PGK1	phosphoglycerate kinase	44 636	9	cytosol	2
DLD1	D-lactate dehydrogenase	62 156	3	mitoch. (IM)	1
YPR004C	probable flavoprotein	36 806	2	mitoch.?	1
IDH2	isocitrate dehydrogenase	37 796	11	mitoch. (Mat)	1
MRF1	mitochondrial respiration factor 1	44 413	12	mitoch. (Mat)	1
ATP1	F1-ATPase subunit α	55 481	5	mitoch. (IM)	1
GAS1	GPI-anchored surface protein	59 556	2	Cell Wall	1
STI1	major stress-response protein	66 251	4	?	1
ENO1	enolase	46 679	8	cytosol	1
TDH3	major isoform of glyceraldehyde-3-phosphate dehydrogenase	35 612	12	cytosol	1
TDH1	minor isoform of glyceraldehyde-3-phosphate dehydrogenase	35 619	13	cytosol	1
GPM2	isoform 2 of phosphoglycerate mutase	35 939	10	cytosol	1
PUS1	pseudouridylate synthase	62 014	2	nucleus	1
UPF3	nonsense mRNA decay protein	44 831	13	nucleus	1
NSP1	nuclear pore major component	86 508	4	nucleus	1

[a] The number of identifications is the number of times the protein was identified by both MALDI and PSD experiments in a discrete band on a second-dimension SDS−PAGE (as shown in Figure 3B), on the basis of independent experiments from three mitochondria preparations. The known or probable localization of the proteins is indicated. For mitochondrial proteins, the sublocalization is also indicated (inner membrane, outer membrane, matrix). The "Band" column refers to the band where the protein is found most often. The "size" column refers to the size of the mature protein, calculated from the gene sequence.

Concerning both aspects, this paper describes the use of nondenaturating electrophoresis to provide the additional evidence of physical contacts between membrane dehydrogenases and with matricial enzymes involved in NADH production.

The first step of this work was the characterization, by a specific staining, of the complexes isolated by nondenaturing colorless electrophoresis (*27*). This led to the identification of a large complex having an intense NADH−Nitro Blue Tetrazolium oxidoreductase activity. This complex was analyzed further from mutant strains inactivated in *GUT2*, *NDE1*, or *NDE2* genes, respectively, to confirm that it actually represents a membrane-bound complex containing intermembrane-facing dehydrogenases. The complex isolated from Δ*gut2* strain still exhibits a high NADH−Nitro Blue Tetrazolium oxidoreductase activity but completely losses the glycerol-3-phosphate-Nitro Blue Tetrazolium oxidoreductase activity (data not shown). The complexes isolated from the individual Δ*nde1* or Δ*nde2* strains do not exhibit significant differences, as compared to the wild-type, but the double Δ*nde1*/Δ*nde2* mutant almost completely losses the NADH−Nitro Blue Tetrazolium oxidoreductase activity. These results unambiguously indicate that these three proteins are part of the complex.

The next step was the identification of other proteins in the complex. After disruption of the complex, discrete bands were obtained by SDS−PAGE. Each of these was cutoff and digested with endo-LysC. The peptide mixture was then analyzed by Edman degradation and further by MALDI-MS.

Among the three proteins expected to be present in the complex, Gut2p and Nde2p were identified by both methods. Nde1p was found in Edman sequencing analyses but not in PSD analyses, showing the resolution limit of the method. This may indicate that this protein is present in a low amount in the complex, as compared to its isoform Nde2p. Luttik et al. (*5*) showed that, in glucose-grown cells, Nde1p was responsible for 80% of the NADH-ubiquinone oxidoreductase activity, Nde2p being responsible for the remaining 20%. In our hands, in lactate-grown cells, individual inactivations of any of these enzymes did not lead to a major alteration of the activity, as measured in situ. The inactivation of both enzymes was required to abrogate the activity. It is possible

that the specific activity of Nde1p is much higher than the specific activity of Nde2p. The difference between observations by Luttik et al. (*5*) and our observations might be an indication of the regulation of the expression of *NDE1* and *NDE2* depending on metabolic conditions.

Both L-lactate-cytochrome *c* oxidoreductase Cyb2p and D-lactate-cytochrome *c* oxidoreductase Dld1p were identified by Edman sequencing and MALDI-MS. Our cells were grown on a mixture of D- and L-lactate and therefore the presence of both enzymes was expected (*33*).

Considering all these results, it can be concluded that the five intermembrane space-facing dehydrogenases (Nde1p, Nde2p, Gut2p, Cyb2p, Dld1p) are associated into the supramolecular complex corresponding to the band at $R_f = 0.44$.

Association of Matricial Enzymes to Matrix-Facing NADH-Dehydrogenase. The complex was also found to contain the matrix-facing NADH-ubiquinone oxidoreductase Ndi1p. This shows an association between the external and the internal dehydrogenases. The three enzymes are very homolog, since *NDE1* and *NDE2* were identified on the basis of this homology to *NDI1* (*5*) and their enzymatic mechanism involves electron transfer from matricial or intermembrane-space NADH to a unique mobile pool of ubiquinone located in the inner membrane.

A particularly interesting observation is the presence of malate dehydrogenase Mdh1p, which was identified by both methods. The mammalian analogue of Mdh1p was found to be tightly associated to the NADH−dehydrogenase complex (*19*). It seems that this functional association is conserved even though the structure of the matrix-facing NADH−dehydrogenase is completely different between yeast and mammals.

Three other enzymes of the tricarboxylic acids cycle were found to be associated. Fumarate hydratase Fum1p catalyzes the metabolic step just before Mdh1p, and was found in the complex, which suggests a channeling between these two enzymes. It should be noted that the presence of Mdh1p and Fum1p is confirmed by both analytical methods. Citrate synthase Cit1p, which catalyzes the metabolic step just after Mdh1p, was frequently identified by the MALDI-MS method. It has been shown that Cit1p is a relatively immobilized protein, strongly suggesting its participation to a complex (*24*). The actual association of Cit1p to a dehydrogenase complex is shown here. The sequencing method revealed the presence of succinate dehydrogenase Sdh1p, which catalyzes the step before Fum1p, but, like Nde1p, it was not identified by the MALDI-MS method.

The association of four enzymes of the TCA cycle to the internal NADH dehydrogenase may be understood as a channeling for matricial NADH. This hypothesis is further supported by the presence of Ald4p as a major component of the complex. Yeast growing on lactate produce large amounts of pyruvate and a large part of pyruvate is decarboxylated to acetaldehyde (by cytosolic pyruvate decarboxylase), which freely diffuses through mitochondrial membrane and is oxidized to acetate by acetaldehyde dehydrogenase Ald4p (*14*). This "acetaldehyde pathway" is one major way for mitochondrial NADH production in aerobic yeast, far over the usual pyruvate dehydrogenase pathway (*14*, *15*). The association of this major NADH-producing enzyme to NADH−dehydrogenase argues for a channeling of matricial NADH.

Two other mitochondrial enzymes were found, which are involved in amino acid metabolism: a probable alanine aminotransferase encoded by ORF *YLR089C*, which synthesizes glutamate from α-ketoglutarate, and Δ1-pyrroline-5-carboxylate dehydrogenase Put2p, which is involved in proline/glutamate conversion. These two enzymes might form a NADH-producing metabolic cluster from α-ketoglutarate (produced in the TCA cycle) to proline. In addition, Put2p, like Ald4p, belongs to the family of aldehydes dehydrogenases. It may be noted that isocitrate dehydrogenase Idh2p, which produces α-cetoglutarate, was also found as a minor component in the complex.

Two New Mitochondrial Dehydrogenases?. A major component of the complex is the product from ORF *YOR356W*, and a minor component is the product from ORF *YPR004C*. This work is the first demonstration that these ORFs actually encode for proteins. Both ORFs were supposed to encode mitochondrial flavoprotein-type oxidoreductases, on the basis of their homology with known components of the mitochondrial electron transport chain. Since the disruption of these ORFs did not lead to an obvious phenotype, their possible substrate is not identified. The gained knowledge that these proteins actually exist opens new perspectives for further studies of these new redox proteins.

The product from one other unknown ORF (*YML128C*) was found in the complex but, in the absence of any additional information, the relevance of this protein to actual mitochondrial localization cannot be ascertained. It should be noted that this protein was found as a major component by both methods.

Size of the Dehydrogenases Complex. CN−PAGE analysis does not allow unambiguous estimation of the size of the complexes, since the mobility of proteins under these conditions depends not only on their mass, but also on their intrinsic charge and on molecular sewing effects. The comparative analysis of oxidative phosphorylation complexes from mammalian mitochondria showed that respiratory complex I, which is heavier than FoF1-ATP synthase, actually exhibited a lower R_f on BN−PAGE, but a higher R_f on CN−PAGE (*34*). In yeast mitochondria, CN−PAGE analysis gives a R_f of 0.44 for the dehydrogenases complex and a R_f of 0.27 for the FoF1-ATP synthase (*27*). It should be noted that the absence of Gut2p, Nde1p or Nde2p (∼60 kDa each) does not result in a significant R_f increase of the dehydrogenases complex (ref *27* and Figure 1 of this paper).

Interaction with Other Mitochondrial Complexes. The dehydrogenases complex seems to contain proteins that are part of other mitochondrial complexes. Hsp60p has been found to be associated namely with ATP synthase (*35*). Since its function is to participate to the assembly of supramolecular complexes, its presence strongly supports the idea that the "dehydrogenase complex" is the result of a coordinated assembly. The presence of Mrf1p, another regulator of the biosynthesis of respiratory complexes (*36*, *37*), also argues for this hypothesis.

Qcr1p and Qcr2p are structural components of respiratory complex III (ubiquinol-cytochrome *c* oxidoreductase) (*38*). Their presence might suggest interactions between the "dehydrogenase complex", among which seven enzymes

reduce ubiquinone (Nde1p, Nde2p, Gut2p, Ndi1p, and Sdh1p and probably YOR356Wp and YPR004Cp), and complex III, which oxidizes ubiquinol. Such an interaction between neighboring complexes has been suggested for complex III and complex IV on the basis of genetic approaches (*39*, *40*) and it is hypothesized that the yeast respiratory chain would be organized as functional macromolecular units (*41*). We observed that the absence of Nde1p, Nde2p or both, resulted in a strong decrease of the amount of complex III, but only in a marginal decrease of complex IV (Table 2), which supports the idea of an interaction between the dehydrogenases complex and complex III, which are connected by the ubiquinone pool.

The presence of Atp1p, as a minor component, might be less functionally relevant. This F1-ATPase subunit is a major mitochondrial protein and might contaminate the dehydrogenases complex. However, several evidences suggest the existence of interactions between respiratory complex IV and ATP-synthase (*42*, *43*). Such interactions might also exist between ATP synthase and other respiratory enzymes. In addition, Atp1p may play a role in the assembly of mitochondrial complexes (*44*).

These data might suggest that, in addition to an organization as a complex, mitochondrial dehydrogenases might have topological relationships with other complexes involved in oxidative phosphorylation.

Alternative Mitochondrial Localization for Cell Wall Proteins?. The complex was also found to contain Gas1p. This protein is attached to the outer leaflet of the plasma membrane by a glycosyl-phosphatidylinositol anchor (*45*) but was localized in the cell wall (*46*). It was recently shown in the laboratory that the so-called "SUN family" proteins Sun4p and Uth1p (*47*, *48*) have a double mitochondria/cell wall localization.[3] A recent work describes the function of cell-wall protein Pir1p in adressing the endonuclease Apn1p to the nucleus or to mitochondria (*49*). The presence of Gas1p in mitochondria may be a further indication that a relatively large number of proteins have double mitochondria/cell wall localization. It should be noted that the product of the putative ORF *YOL132W* (also known as Gas4p), which exhibits strong homologies to Gas1p (*50*), was found in another mitochondrial complex.[4]

MALDI-MS as a Tool for the Study of Protein Complexes. The methodology developed in the present paper is a powerful tool for the identification of possible physical contacts between proteins. Electrospray mass spectrometry identifications have been used to identify components of supramolecular arrangements such as ribosomes (*51*), proteasome (*52*), and spliceosome (*53*) and developping methods will soon allow to access complexes organization and assembly (see ref *54* for a review*)*. Until now, most information has been obtained on soluble and well-identified complexes, of which the components can be separated by classical 2D-electrophoresis (isoelectrofocusing/SDS). However, proteins participating to membrane-associated complexes are often too hydrophobic to be separated by isoelectrofocusing and are therefore out of the scope of systematic functional genomics analyses.

Because the gel bands observed in the second dimension electrophoresis most often contained more than one protein, peptide mixtures resulting from the corresponding proteolytic digests were highly complex. Thus, automated Edman degradation could only be applied to fractions corresponding to single peaks collected after reversed-phase chromatographic separation. This procedure of protein identification turned out to be too time consuming, although it led to several unambiguous identifications, including that of Nde1p. MALDI mass spectrometry allowed us to fulfill the identification task within a two-step procedure that was strictly observed. Indeed, two separate searches were conducted. The first search, performed with a set of monoisotopic peptide masses (MSFit search engine), usually led to a list of several probable proteins. At this stage, only proteins matching the molecular weight estimated from the second dimension SDS−PAGE experiment were taken into account. In a second step, peptide peaks corresponding to top ranked protein candidates were chosen for post source decay (PSD) fragment ion analysis. The second search was then performed separately with the observed PSD fragment ion masses from these selected precursors (MSTag search engine). Immonium ions observed on PSD spectra were used to check the results of this second query. All herein reported protein identifications followed this complete procedure and resulted from an unique answer with the two separate database searches. The major limitation of this procedure relying on MALDI mass spectrometry lies in the resolution of the ion gate used to select precursor ions for PSD analysis: with our instrument, precursor ions had to be separated by more than 15 mass units to allow proper fragmentation analysis.

To our knowledge, this procedure led to the first data obtained on a membrane-associated complex that had not been identified before. This opens new possibilities about the identification of new components associated to other membrane complexes.

Contaminating Proteins. Several proteins, which do not seem to be relevant to inner mitochondrial membrane/matricial localization were identified and might be contaminants of this fraction. However, their identification in a high molecular weight complex on nondenaturing CN−PAGE is a good indication that they could be associated together.

A first group is formed by major cellular proteins, which contaminate nearly all cellular fractions: isoforms I and III of glyceraldehyde-3-phosphate dehydrogenases (Tdh1p and Tdh3p), isoform 2 of phosphoglycerate mutase Gpm2p, phosphoglycerate kinase Pgk1p, enolase Eno1p, phosphoenolpyruvate carboxykinase Pck1p, pyruvate decarboxylase Pdc1p, acetyl-coA hydrolase Ach1p, endoplasmic reticulum-membrane proteins Sso1p and Sso2p, and outer mitochondrial membrane proteins OM45p and Tom70p. All these proteins are frequently found in MALDI-MS identifications due to their high natural abundance.

The second group of proteins has a known nuclear localization: nucleoporin Nsp1p, methyladenine glycosylase Mag1p, nonsense mRNA regulator Upf3p, pseudouridylate synthase I Pus1p, and a putative ATPase Pch2p. Nuclei are minor contaminants of mitochondria preparation, and major nuclear components might thus be detected, due to the high sensitivity of MALDI-MS.

This problem of detection of probable contaminating proteins is an obvious limit of the experimental protocol used

[3] N. Camougrand et al., unpublished data.
[4] X. Grandier-Vazeille et al., unpublished data.

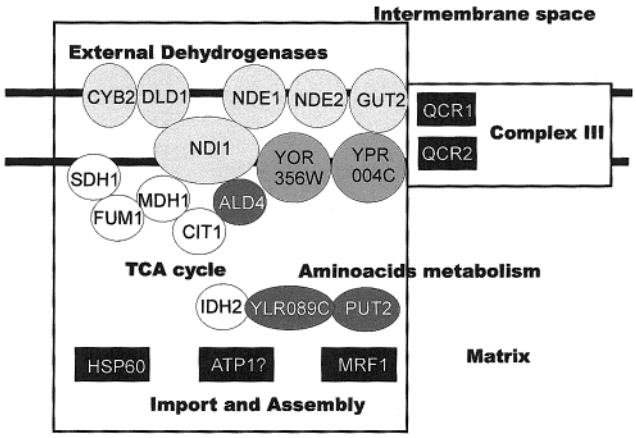

FIGURE 5: Schematic representation of the components of the dehydrogenase complex. Membrane dehydrogenases are indicated in light gray. The sub-localization of putative dehydrogenases YOR356Wp and YPR004Cp is arbitrary. TCA cycle enzymes are indicated in white with the localization of Sdh1p close to the membrane. Enzymes involved in amino acids metabolism may form a metabolic cluster with Idh2p. Ald4p, which is a major producer of NADH, might be associated to Ndi1p. Proteins possibly involved in the assembly and organization of the complex and proteins of complex III, which might interact with the Dehydrogenases complex, are indicated in black.

in this work. The protocol, which includes extensive washing steps of mitochondrial fraction, was optimized to limit such contaminations, but major proteins cannot be completely eliminated. Quantitative methods of mass spectrometry (see ref *53* for review) may partially answer to this problem, but a major cellular protein organized into a large oligomer, such as Tdh3p, is a potential contaminant of all cellular fractions. The repetition of experiments made under different conditions, and the combination of different approaches can unambiguously establish the participation of a protein to a complex. It should be noted that, as discussed above for cell wall proteins, some of the proteins we considered as "contaminants" might actually have a double localization.

CONCLUSION

As a conclusion, the procedure developped in this paper strongly supports the hypothesis of the existence of a mitochondrial dehydrogenase complex, which contains the five intermembrane space-facing dehydrogenases, the matrix-facing NADH dehydrogenase, a part of the TCA cycle and an additional NADH-producing enzyme (Figure 5). We also obtained additional information about potential interactions between this complex and other mitochondrial complexes, namely bc1-complex. An additional aspect of this work is the identification of possible alternative mitochondrial localization for some cell wall proteins.

The sensitivity of the method, although having drawbacks such as the identification of probably contaminating proteins, is a powerful tool for the identification of physiological interactions between proteins. It should be noted that classical methods used to detect protein−protein interactions, such as co-immunoprecipitation or dihybrid system, did not allow, to our knowledge, the identification of dynamic interactions such as those probably involved in metabolic channeling. The method can now be applied to a metabolic analysis. For instance, the interaction of Ald4p with Ndi1p may be critical in cells grown on lactate, but might be less important on cells grown aerobically on glucose, where pyruvate dehydrogenase should be the main pathway for pyruvate oxidation. This type of information will contribute to a dynamic view of yeast metabolism.

REFERENCES

1. Friedrich, T., Abelmann, A., Brors, B., Guenebaut, V., Kintscher, L., Leonard, K., Rasmussen, T., Scheide, D., Schlitt, A., Schulte, U., and Weiss, H. (1998) *Biochim. Biophys. Acta 1365*, 215−219.
2. De Vries, S., and Grivell, L. A. (1988) *Eur. J. Biochem. 176*, 377−384.
3. Marres, C. A., de Vries, S., and Grivell, L. A. (1991) *Eur. J. Biochem. 195*, 857−862.
4. Small, W. C., and McAlister-Henn, L. (1998) *J. Bacteriol. 180*, 4051−4055.
5. Luttik, M. A. H., Overkamp, K. M., Kötter, P., de Vries, S., van Dijken, J. P., and Pronk, J. T. (1998) *J. Biol. Chem. 273*, 24529−24534.
6. Ouhabi, R., Rigoulet, M., Lavie, J. L., and Guérin, B. (1991) *Biochim. Biophys. Acta 1060*, 293−298.
7. Fitton, V., Rigoulet, M., Ouhabi, R., and Guérin, B. (1994) *Biochemistry 33*, 9692−9698.
8. Avéret, N., Fitton, V., Bunoust, O., Rigoulet, M., and Guérin, B. (1998) *Mol. Cell. Biochem. 184*, 67−79.
9. Manon, S. (1999) *Biochim. Biophys. Acta 1410*, 85−90.
10. Larsson, C., Pahlman, I. L., Ansell, R., Rigoulet, M., Adler, L., and Gustafsson, L. (1998) *Yeast 15*, 347−357.
11. Guiard, B. (1985) *EMBO J. 4*, 3265−3272.
12. Lodi, T., and Ferrero, I. (1993) *Mol. Gen. Genet. 238*, 315−324.
13. Pronk, J. T., Wenzel, T. J., Luttik, M. A., Klaassen, C. C., Scheffers, W. A., Steensma, H. Y., and van Dijken, J. P. (1994) *Microbiology 140*, 601−610.
14. Boubekeur, S., Bunoust, O., Camougrand, N., Castroviejo, M., Rigoulet, M., and Guérin, B. (1999) *J. Biol. Chem. 274*, 21044−21048.
15. Overkamp, K. M., Bakker, B. M., Kotter, P., van Tuijl, A., de Vries, S., van Dijken, J. P., and Pronk, J. T. (2000) *J. Bacteriol. 182*, 2823−2830.
16. Fukushima, T., Decker, R. V., Anderson, W. M., and Spivey, H. O. (1989) *J. Biol. Chem. 264*, 16483−16488.
17. Spivey, H. O. (1991) *J. Theor. Biol. 152*, 103−107.
18. Ushiroyama, T., Fukushima, T., Styre, J. D., and Spivey, H. O. (1992) *Curr. Top. Cell. Regul. 33*, 291−307.
19. Ovadi, J., Huang, Y., and Spivey, H. O. (1994) *J. Mol. Recognit. 7*, 265−272.
20. Beeckmans, S., Driessche, V. E., and Kanarek, L. (1989) *Eur. J. Biochem. 183*, 449−454.
21. Robinson Jr, J. B., Inman, L., Sumegi, B., and Srere, P. A. (1987) *J. Biol. Chem. 262*, 1786−1790.
22. Lindbladh, C., Rault, M., Hagglund, C., Small, W. C., Mosbach, K., Bülow, L., Evans, C., and Srere, P. A. (1994) *Biochemistry 33*, 11692−11698.
23. Morgunov, I., and Srere, P. A. (1998) *J. Biol. Chem. 273*, 29540−29544.
24. Haggie, P. M., and Brindle, K. M. (1999) *J. Biol. Chem. 274*, 3941−3945.
25. Velot, C., and Srere, P. A. (2000) *J. Biol. Chem. 275*, 12926−12933.
26. Patrikian, A., Olvecsky, B., Swaminathan, R., Li, Y., and Verkman, A. S. (1998) *J. Cell. Biol. 140*, 821−829.
27. Grandier-Vazeille, X., and Guérin, M. (1996) *Anal. Biochem. 15*, 248−254.
28. Law, R. H. P., Manon, S., Devenish, R. J., and Nagley, P. (1995) *Methods Enzymol. 260*, 133−163.
29. Rosenfeld, J., Capdevielle, J., Guillemot, J. C., and Ferrara, P. (1992) *Anal. Biochem. 203*, 173−179.
30. Tzagoloff, A., and Myers, A. M. (1986) *Annu. Rev. Biochem. 55*, 249−285.
31. Kawasaki, H., Emori, Y., and Suzuki, K. (1990) *Anal. Biochem. 191*, 332−336.

32. Shägger, H., and Pfeiffer, K. (2000) *EMBO J. 19*, 1777−1783.
33. De Vries, S., and Marres, C. A. M. (1987) *Biochim. Biophys. Acta 895*, 205−239.
34. Shägger, H., Cramer, W., and von Jagow, G. (1999) *Anal. Biochem. 217*, 220−230.
35. Gray, R. E., Grasso, D. G., Maxwell, R. J., Finnegan, P. M., Nagley, P., and Devenish, R. J. (1990) *FEBS Lett. 268*, 265−268.
36. Pel, H. J., Maat, C., Rep, M., and Grivell, L. A. (1992) *Nucleic Acids Res. 20*, 6339−6346.
37. Yamazoe, M., Shirahige, K., Rashid, M. B., Kaneko, Y., Nakayama, T., Ogasawara, N., and Yoshikawa, H. (1994) *J. Biol. Chem. 269*, 15242−15252.
38. Hunte, C., Koepke, J., Lange, C., Rossmanith, T., and Michel, H. (2000) *Struct. Fold. Des. 15*, 669−684.
39. Hamel, P., Lemaire, C., Bonnefoy, N., Brivet-Chevillote, P., and Dujardin, G. (1998) *Genetics 150*, 601−611.
40. Cruciat, C. M., Brunner, S., Baumann, F., Neupert, W., and Stuart, R. A. (2000) *J. Biol. Chem. 275*, 18093−18098.
41. Bouman, H., Grivell, L. A., and Berden, J. A. (1998) *J. Biol. Chem. 273*, 4872−4877.
42. Kermorgant, M., Bonnefoy, N., and Dujardin, G. (1997) *Curr. Genetics 31*, 302−307.
43. Boyle, G. M., Roucou, X., Nagley, P., Devenish, R. J., and Prescott, M. (1999) *Eur. J. Biochem. 262*, 315−323.
44. Yuan, H., and Douglas, M. G. (1992) *J. Biol. Chem. 267*, 14697−14702.
45. Nuoffer, C., Jeno, P., Gonzelmann, A., and Riezman, H. (1991) *Mol. Cell. Biol. 11*, 27−37.
46. De Sampaïo, G., Bourdineaud, J. P., and Lauquin, G. J. M. (1999) *Mol. Microbiol. 34*, 247−256.
47. Mouassite, M., Camougrand, N., Schwob, E., Demaison, G., Laclau, M., and Guérin, M. (2000) *Yeast 16*, 905−919.
48. Camougrand, N., Mouassite, M., Velours, G., and Guérin, M. (2000) *Arch. Biochem. Biophys. 375*, 154−160.
49. Vongsamphanh, R., Fortier, P. K., and Ramotar, D. (2001) *Mol. Cell. Biol. 21*, 1647−1655 .
50. Caro, L. H., Tettelin, H., Vossen, J. H., Ram, A. F., Van den Hende, H., and Klis, F. M. (1997) *Yeast 13*, 1477−1489.
51. Link, J., Eng, J., Schieltz, D. M., Carmack, E., Mize, G. J., Morris, D. R., Garvik, B. M.; Yates J. (1999) *Nat. Biotechnol. 17*, 676−682.
52. Verma, R., Chen, S., Feldman, R., Schieltz, D., Yates, J., Dohmen, J., and Deshaies, R. J. (2000) *Mol. Cell. Biol. 11*, 3425−3439.
53. Bouveret, E., Rigaut, G., Shevchenko, A., Wilm, M., and Séraphin, B. (2000) *EMBO J. 19*, 1661−1671.
54. Miranker, A. D. (2000) *Curr. Opin. Struct. Biol. 10*, 601−606.

BI010277R